Photoinduced autofluorescence modifications of cells in an optical trap

Karsten König[1,2], Yagang Liu[1,3], Greg J. Sonek[3], Michael W. Berns[1], Bruce J. Tromberg[1]

[1]Beckman Laser Institute and Medical Clinic, University of California, Irvine, CA 92715
[2]Institute of Laser Technologies in Medicine, D-89081 Ulm, Germany
[3]Department of Electrical and Computer Engineering, University of California, Irvine, CA 92715

1. ABSTRACT

Photoinduced modifications of NAD(P)H attributed autofluorescence of CHO cells in a single-beam gradient force optical trap (optical tweezers) were studied. Fluorescence spectra of single cells in the optical trap were measured using a modified microscope with an IR microbeam at 1064 and 760 nm for trapping, UVA radiation at 365 nm for fluorescence excitation, and an optical multichannel analyzer for spectral recording. No strong effect of the 1064 nm trapping beam on fluorescence intensity and spectral characteristics was found, even for power densities up to 70 MW/cm^2. In contrast, 760 nm microirradiation resulted in a significant fluorescence increase, probably indicating cell damage due to absorption by heme-containing molecules. UVA exposure (1 W/cm^2) of the trapped cells generated within seconds an initial fluorescence decrease, followed by a significant increase up to 5X of the value prior to irradiation. The UVA-induced modifications reflect NAD(P)H autooxidation and irreversible cell damage due to oxidative stress.

2. INTRODUCTION

Optical trapping of microscopic objects, also called optical tweezers, is a novel technique which utilizes radiation pressure generated by laser microbeams[1]. Ashkin[2] first introduced the single-beam gradient force optical trap consisting of a laser beam focused to a diffraction-limited spot, d, by a high numerical aperture (NA) microscope objective (see Fig. 1), where $d \approx \lambda/NA$.[3] Cells can be drawn into and trapped in the focal spot. This is due to the change in momentum that occurs when the microbeam interacts with a single cell, resulting in forces which are sufficient to "catch", hold and manipulate a cell or organelle in an optical "potential well" (see Fig. 2). These forces, F, can be determined by F=QP/c, where c is the velocity of light in medium, and Q an efficiency parameter which depends on the optical properties of the trapped object and laser beam quality. Trapping forces are in the range of pN for typical trapping powers of 50-500 mW. In order to reduce radiometric forces and avoid thermal damage, the wavelength of the trapping beam, λ, should be in the near-infrared (NIR) "optical window" where biological samples absorb poorly.

Table I summarizes light dose parameters typically used during cell trapping with a 100 mW NIR beam focused by a 100x, NA=1.2 objective. As shown, cells are exposed to intensities in the range of MW/cm^2 (10^6 W/cm^2) and, in the course of a 10 min experiment, radiant exposures can be as high as GJ/cm^2 (10^9 J/cm^2).

Table I Typical optical trapping parameters

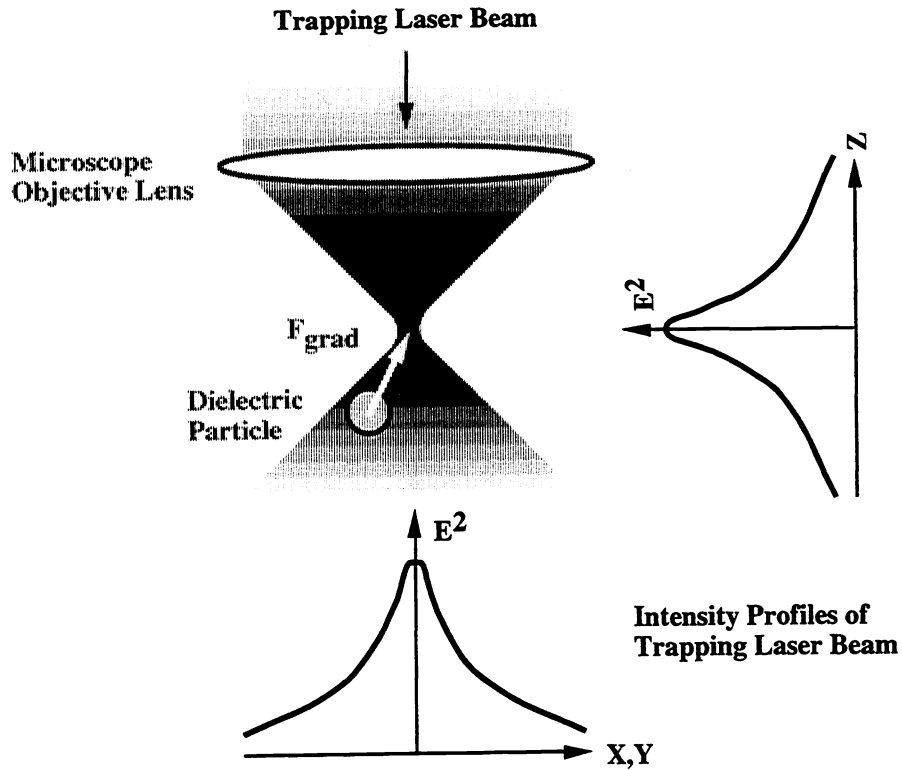| wavelength nm	power mW	trapping time min	spot size µm	intensity MW/cm^2	radiant exposure GJ/cm^2
760	100	10	0.63	31	19
1064	100	10	0.89	16	10

Fig. 1 Single-beam gradient force optical trap.
Transverse, as well as axial forces, pull the polarized dielectric cell towards the beam spot.
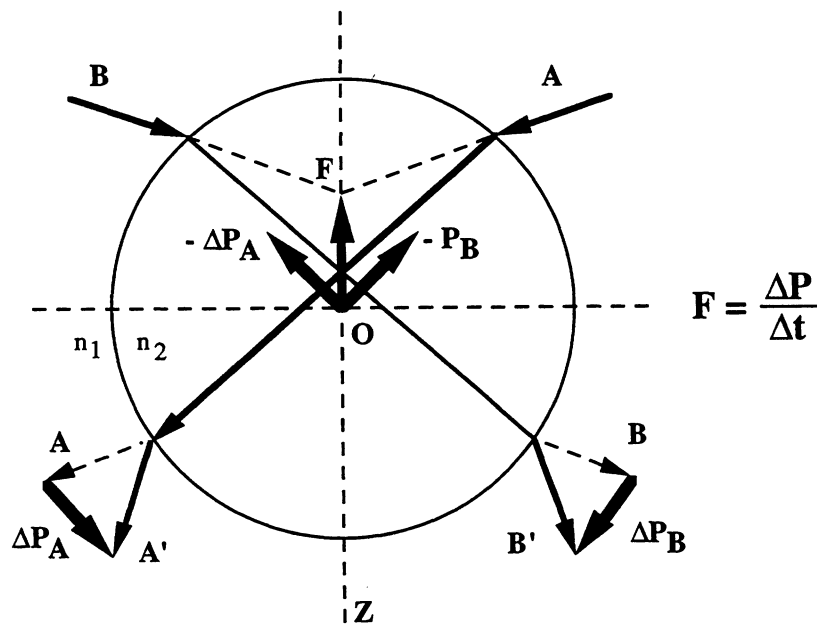

$$F = \frac{\Delta P}{\Delta t}$$

Fig. 2 Ray-optics model for generation of optical forces.
The deflection of light along the pathways A and B results in change of momentum p and therefore, in force generation (F=dp/dt).
Backward forces F are created in the case of cell localizations beyond the focal point.
For simplicity, reflected rays are not considered.

This enormous photon flux may place cells in a state of stress by inducing mechanical, thermal, and chemical changes that affect cellular metabolism. One method for obtaining information on light-induced disturbances to metabolic function is monitoring intracellular fluorescence of the reduced coenzymes β-nicotinamide adenine dinucleotide (NADH) and β-nicotinamide adenine dinucleotide phosphate (NADPH). These fluorescent coenzymes (NADH, NADPH, flavins) act as highly sensitive bioindicators of metabolic function. This was first recognized by Chance et al.[4] who studied intracellular oxygen status by means of non-destructive NADH fluorometry. An increase in NADH fluorescence has been found during ischemia, hypoxia, and anoxia in the brain[5]. Lohmann et al.[6] used the 365 nm excited autofluorescence for tumor detection. Differences in fluorescence intensities of yeast strains and human fibroblasts were correlated with the function of the mitochondrial respiratory chain[7,8]. Fluorescence changes were also used as a method to detect cellular and tissue damage[9].

NADH, NADPH, and flavin coenzymes act as hydrogen (electron)-transferring molecules in the respiratory chain. The hydrogen uptake at position 4 of the pyridine ring (Fig. 3) results in significant spectral changes. In particular, a new absorption band at 340 nm appears. Excitation of this electronic transition results in fluorescence emission around 460 nm in aqueous solution. The reduced coenzymes possess a folded and an unfolded configuration. The unfolded form, which is typical for bound coenzymes, shows a blue-shifted maximum. The oxidized forms NAD and NADP fluoresce at around 445 nm with a 1000 fold reduction in fluorescence yield in comparison to the reduced forms (excitation: >300 nm). Therefore, UVA-excited cellular autofluorescence can be attributed to the reduced forms of the pyridine coenzymes.
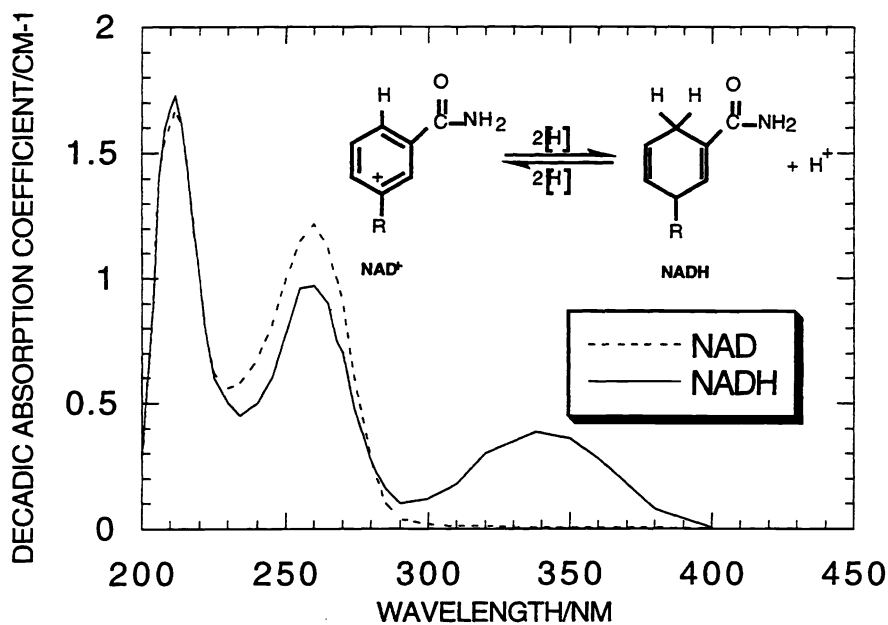

Fig. 3 Structure and absorption spectra of NAD/NADH (64 μM, PBS)

In this paper we describe intracellular autofluorescence variations recorded from single cells in an optical trap during light stress. In particular, the influence of NIR trapping radiation (1064 nm, 760 nm) and fluorescence excitation radiation (365 nm) were investigated. Our results show that in contrast to 1064 nm, radition at 760 and 365 nm was found to induce changes in the cellular redox state. We suggest that endogenous absorbers such as coenzymes and enzymes with a tetrapyrrolic prosthetic group may be responsible for these and previously-reported microirradiation effects[10].
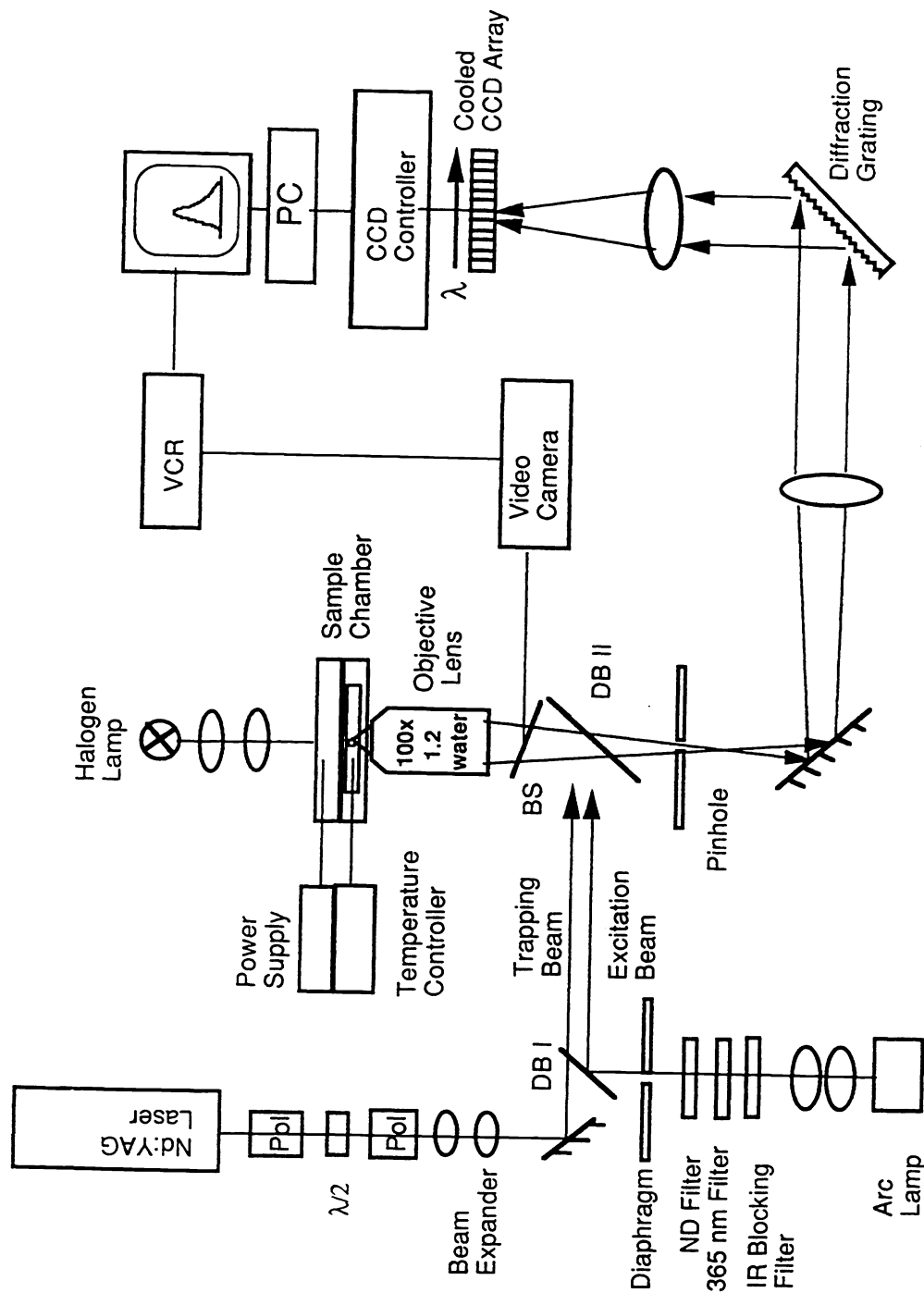
Fig. 4 Experimental set-up for fluorescence spectroscopy on optically-trapped CHO cells. The beamsplitter BS reflects visible and IR light either to an eyepiece equipped with an IR blocking filter, or to a video camera for monitoring cell trapping, cell size, and position of the trapped cell within the fluorescence detection area. The dichroic mirror (DB II) inside the microscope reflects both the IR trapping radiation and the UV excitation, and transmits fluorescence radiation at wavelengths >400 nm.

3. MATERIALS AND METHODS

Chemicals. NADH and NADPH were obtained from Sigma in preweighed glass vials. The reduced coenzymes were dissolved in PBS, pH= 7.4, and promptly used. Alcohol dehydogenase (ADH, Sigma) was used in a final concentration of 10 μM.

Cell and cell culture. Chinese hamster (Cricetulus griseus) ovary cells (CHO, ATCC no. 61) were maintained in GIBCO's minimum essential medium (MEM, 10% fetal bovine serum). Cells were subcultured in T-25 tissue culture flasks twice a week using 0.25% trypsin for dessication. For experimentation, dessicated cells were diluted in calcium- and magnesium-free PBS, pH= 7.4, and injected into a modified Rose culture chamber[11] . Experiments were carried out mostly at 25°C.

Experimental set-up. The scheme of the modified microscope for laser-induced optical trapping and microspectrofluorometry is shown in Fig. 4. The trapping beam was provided by a continuous-wave Nd:YAG laser operating at 1064 nm in the TEM_{00} mode. The beam was coupled to an inverted 760 mm Nikon microscope and focused onto the specimen plane by a Leitz 100x objective (NA=1.2, water immersion). The actual *in situ* NIR power reaching the sample was determined by measuring the laser power at the focal plane of the objective, and applying a correction factor[12] that accounts for the different refractive indices. For a measured spot size[12] of 0.9-1.0 mm, a corrected *in situ* power of 200 mW at the sample resulted in an IR intensity of about 30 MW/cm^2. A 200 W high-pressure mercury arc lamp equipped with a dichroic mirror to eliminate IR radiation and an interference filter at 365±25 nm was used as the fluorescence excitation source. Irradiation time was controlled by a computer-driven electronic shutter. A power of 6 μW was measured after the objective (no immersion agent). Considering differences in refractive indices, an *in situ* power of 10 μW was estimated. The focused spot diameter of about 35 μm was determined by the processed fluorescence image of a Rhodamine solution injected into the Rose culture chamber. Thus, a UV radiation intensity of about 1 W/cm^2 was applied.

Fluorescence was collected by the same objective and directed to the entrance slit of a polychromator (300 g/mm grating). An adjustable pinhole at the image plane of the objective allowed fluorescence detection of small sample areas (typically 15 μm in diameter). Spectra were recorded (370-615 nm) with a cooled CCD camera (Princeton Instruments, model TE576/ST135, Trenton, NJ) and analyzed by a personal computer. Each spectrum was acquired in 1s and up to 1200 spectra per cell were measured. Spectral correction factors were obtained by means of a calibrated light source.

For studies with a 760 nm trapping beam, another experimental set-up with a tunable Ti:sapphire laser and a modified confocal laser scanning microscope (Zeiss, Germany) equipped with the cooled CCD camera was used. Assuming a diffraction-limited spot size, an IR intensity of 50 MW/cm^2 (160 mW) was estimated.

4. RESULTS

4.1. Modifications of UV excited fluorescence of aqueous NAD(P)H solution

Initial fluorescence studies were performed on coenzyme solutions using the same set-up as for cell studies, but with the reduced diameter of detection area of 10 μm which corresponds to the average cell size. NADH and NADPH fluorescence was observed with a main peak at 457 nm, whereas NADH-ADH mixtures exhibited a maximum at 442 nm. The fluorescence quantum yield of the NADH-ADH mixture was a factor of two higher than protein-free solution (Fig. 5a).

The dependence of fluorescence intensity on concentration is depicted in Fig. 5b. Application of UV excitation (300 J/cm^2) to a 0.1 mg/ml solution for 5 min resulted in a fluorescence decrease of only 5%, indicating that no significant photobleaching of free NADH occurs. In addition, 1064 nm light was applied for 30 min without any fluorescence reduction.

4.2. Determination of minimum trapping power

Cells were trapped at 1064 nm with an *in situ* power of 230 mW, and raised to a height of about 10 μm above the glass bottom to avoid cell attachement. In order to determine the minimum laser power required for trapping, the laser power was step-wise (in the critical range: every 2 mW) diminished by rotation of the polarizer and the sample chamber slowly translated along one horizontal axis. When the cell could no longer be held by the laser, this power defined the minimum trapping power. We investigated 10 cells and found a cell size of 11.0±1.9 μm and a minimum trapping power of 28.1±4.4 mW. Of course, much higher powers are necessary to confine a motile cell in the trap. Therefore, 100, 230, and 460 mW were chosen for autofluorescence monitoring during cell trapping.
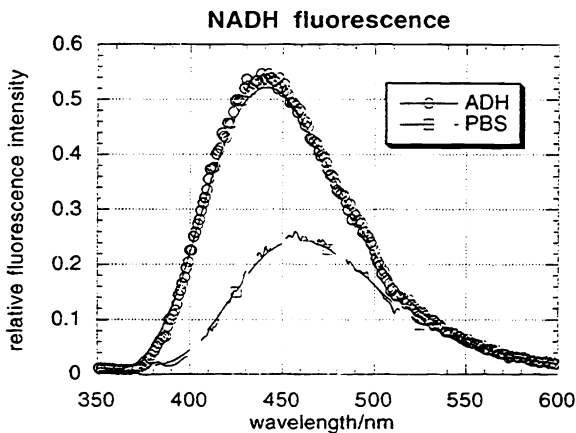

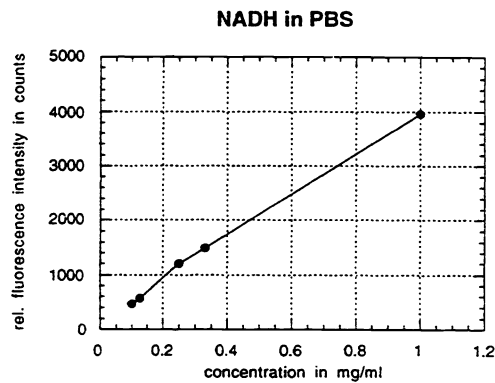Fig. 5a Fluorescence of free 0.1 mM NADH and bound NADH (NADH-ADH mixture) in PBS

Fig. 5b Fluorescence intensity of free NADH in dependence on concentration. Background intensity (PBS-filled chamber): 2000±100 counts.

4.3. Autofluorescence during 1064 nm exposure

4.3.1. Autofluorescence of laser-trapped and glass attached cells

The autofluorescence of 20 trapped cells for the power levels of 100 mW, 230 mW, and 460 mW each was measured immediately (about 5 s) after the start of trapping (Table II). For comparison, cells that were attached to the chamber coverslip and not exposed to the 1064 nm laser beam, were also measured. Non-trapped cells started to attach to the lower glass surface within minutes. No dependence of fluorescence intensity on trapping power was found. The mean standard deviation of about 30% indicates a high variance in the concentration of the endogenous fluorophores. Cells showed generally a higher fluorescence intensity with increasing size. No substantial autofluorescence difference existed between laser-trapped and unexposed cells. All cells showed a fluorescence maximum at around 455 nm.

Table II Autofluorescence signals of laser-trapped cells compared with glass-attached cells (0 mW). Errors indicate sample standard deviation.

power	0 mW	100 mW	230 mW	460 mW
fluorescence intensity	534±172	558±169	519±201	493±173

4.3.2. Time-dependent fluorescence modifications of laser-trapped cells

In order to acquire information on autofluorescence changes from cells trapped for extended periods of time, fluorescence signals were monitored for 20 min (trap power = 460 mW, λ = 1064 nm) and compared with those of glass-attached cells. To minimize UV-induced effects, the only 8 spectra were recorded at 0, 1, 4, 7, 10, 13, 16, and 20 min,. Some cells, mainly those that were optically-trapped, showed a fluorescence increase. However, the highest detectable intensity was only 20% greater than the initial value. In general, glass-attached cells showed a behavior comparable to those of the rapped cells (Fig. 6). No morphological damage was obvious during trapping.

In another study, 10 cells were chosen to be trapped for a period of one hour (trap power = 230 mW, λ = 1064 nm). Cell fluorescence was recorded every 10 min. Two samples showed a 50% fluorescence increase. However, this was caused by the sudden incorporation of an additional cell in the same trap. Two other cells exhibited a significant fluorescence decrease concomitant with cell lysis. The remaining cells did not change their fluorescence intensity significantly as shown in Fig. 7.
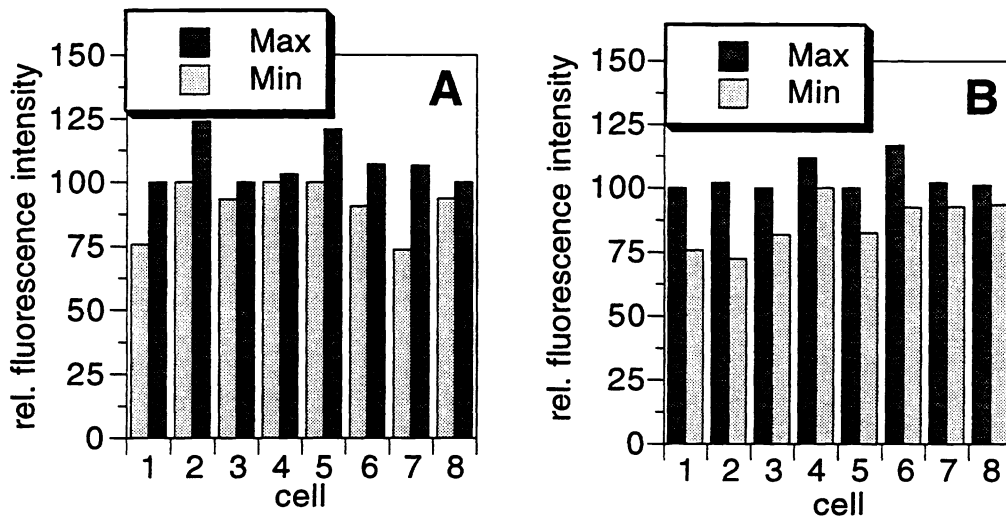
Fig. 6. Relative fluorescence extrema of cells trapped for 20 min (A) compared with control (B).

4.3.4. Autofluorescence during 760 nm exposure

Ten cells were trapped with a constant light intensity of about 50 MW/cm^2 and autofluorescence was recorded in time intervals of 5 min. Nine cells exhibited a significant fluorescence increase with trapping time. As demonstrated in Fig.7, up to a factor of two increase in fluorescence intensity was observed at 22 min (66 GJ/cm^2). One cell showed no significant changes.
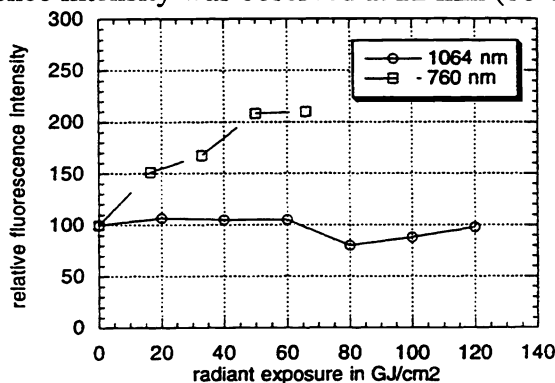
Fig. 7 Fluorescence of long-term trapped cells with 1064 nm and 760 nm microbeam

4.3.5. Autofluorescence modifications of UV-stressed cells

The following studies were carried out to investigate the influence of UV exposure; in particular, the influence of the fluorescence excitation radiation. Ten cells were trapped (460 mW) for 10 min and than, in the optical trap, permanently exposed to 365 nm light of the mercury lamp. Simultaneously, a series of 100 fluorescence spectra were recorded. Each series takes 120 s (100 s detection time, 20 s read-out time) and corresponds to an applied radiant exposure of 100 J/cm^2. The dark period between each series was 5 s. For comparison, glass-attached cells (no IR exposure) were used.

As demonstrated in the fluorescence kinetics curves shown in Figs. 8 and 9, autofluorescence changes dramatically during UV exposure. During the first exposure phase, the fluorescence intensity rapidly decreased. A fading parameter (radiant exposure where the fluorescence intensity at 450 nm dropped to 37% of the initial value, I_0) of about 100 J/cm^2 was determined. Interestingly, a minimum autofluorescence intensity occurred at about this radiant exposure, followed by a significant fluorescence increase during further exposure (the second exposure phase). Fluorescence levels from the last spectrum of each series were lower than the intensities seen in the first spectrum of the following series. This jump is suggestive of dark reactions. In the third exposure phase, the fluorescence of the permanently exposed cell achieved a maximum. In the case of the cell in figures 8 and 9, this maximum was about 2.5 fold the initial value I_0, and was achieved after 12 min ($\approx$700 J/cm^2). In order to determine whether this maximum is indicative of an equilibrium between the fading rate and rate of fluorescence increase, the cell was maintained in the dark for 10 min. A final series of 100 spectra (numbers 800-900) was subsequently recorded. Indeed, a new fluorescence maximum with a 4.5X higher value than I_0 was observed. Following this recording, the intensity decreased within 120 s to a value close to the maximum obtained prior to the dark phase. In addition to modifications in fluorescence intensity, a red shift of the fluorescence maximum and a decreased ratio of 440 nm (protein-bound peak) to 460 nm (un-bound peak) were observed.

The main parameters of UVA-induced fluorescence modifications are summarized in Table III and IV. All cells showed the same fluorescence behavior. However, laser-trapped cells tended to achieve earlier, higher fluorescence maxima than non-trapped cells. Four out of 20 cells exhibited obvious morphological damage. At a radiant exposure of 270 J/cm^2, the laser-trapped cell #4 (Table III) showed a sudden significant increase in fluorescence by nearly a factor of 5 within 2 seconds, concomitant with cell rupture. The increase was followed by a slow fluorescence decrease.
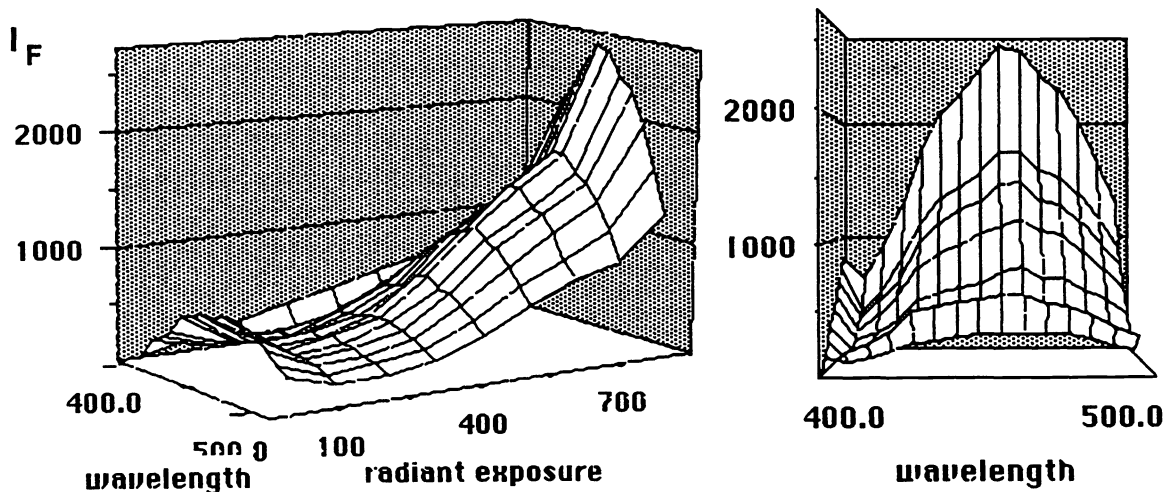

Fig. 8   Modifications of the autofluorescence spectrum of a single cell during UVA exposure. Plots contain data of spectrum 1 (1 J/cm^2), 101, 201, 301, 401, 501, 601, 701, and 801 (801 J/cm^2). Spectrum 801 was obtained after a dark phase of 10 min.
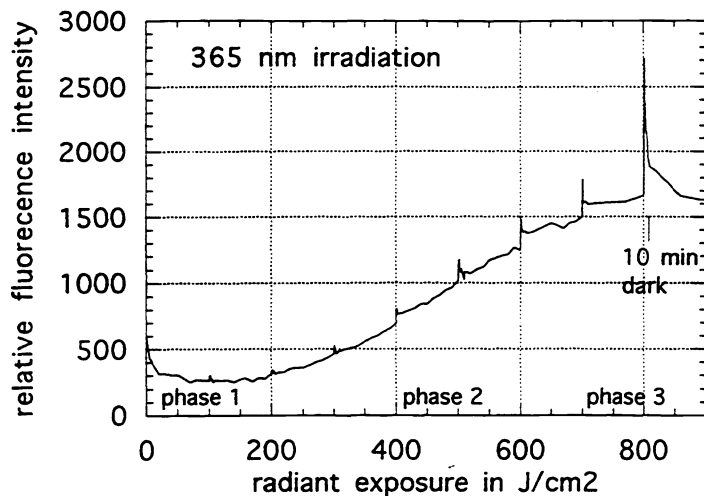
Fig. 9 UVA-induced fluorescence modifications at 460 nm

Table III Effect of UV stress on laser-trapped cells.

I_{10}: intensity after 10 min trapping, I_0: initial intensity, $t_{min}(t_{max})$: time where minimum (maximum) during exposure occurred, $I_{min}(I_{max})$: rel. minimum (maximum) intensity during exposure, I_{dark}: intensity after dark period, def: defective cells

cell	I_{10}/I_0 (%)	t_{min} (s)	I_{min}/I_0 (%)	t_{max} (s)	I_{max}/I_0 (%)	I_{dark}/I_0 (%)
1	94.0	110	40.8	700	310.4	425.7
2	94.2	100	25.1	700	234.5	542.8
3	106.1	110	34.0	600	149.5	def.
4	87.3	100	23.7	240 ?	90.8	def.
5	92.3	100	39.7	800	187.6	335.3
6	87.5	100	35.5	600	143.4	310.1
7	110.2	200	24.1	700	190.1	411.0
8	103.1	150	23.4	750	177.7	370.2
9	98.2	200	20.9	700	103.8	547.7
10	92.2	320	20.7	1050	186.5	496.8
mean	**96.5± 7.7**	**149± 72**	**28.8± 7.8**	**733± 135**	**177± 63**	**430± 91**

Table. IV Autofluorescence kinetics of UVA-exposed, glass-attached cells (no IR exposure)

cell	t_{min} (s)	I_{min}/I_0 (%)	t_{max} (s)	I_{max}/I_0 (%)	I_{dark}/I_0 (%)
1	240	37.7	720	310.4	554.3
2	120	40.8	550	234.5	314.5
3	150	37.2	840	149.5	252.1
4	120	35.8	960 ?	90.8	150.6
5	400	29.6	1100	187.6	234.8
6	360	23.6	1080	143.4	192.2
7	220	28.5	903	190.1	231.0
8	120	30.4	1020	177.7	118.8 def
9	360-	27.3	1320	103.8	149.3
10	350	23.4	1440	186.5	94.9 def
mean	**244± 115**	**31.4± 6.1**	**993± 265**	**177± 63**	**260± 131**

5. DISCUSSION

UVA excitation of CHO cells results in a broad-band fluorescence emissions with a maximum typical for the reduced coenzyme NADH. Indeed, sensitive fluorescence microscopy on CHO cells showed that the preferential intracellular sites of UVA-excited autofluorescence are mitochondria (data not shown). The autofluorescence intensity of trypsinized CHO cell suspensions corresponds to the fluorescence of 0.1 mM free NADH in aqueous solution. Taking into account the fact that bound NADH exhibits up to a 3 fold increase in fluorescence intensity, an intracellular NAD(P)H concentration between 30 μM and 100 μM can be estimated. This value corresponds with data from the literature[13,14].

Autofluorescence spectroscopy during cell trapping with a 1064 nm microbeam did not produce significant modifications to autofluorescence spectral characteristics. Due to the lack of efficient absorbers in this spectral region, no thermal-induced damage is expected even for tightly focused radiation that results in power densities in the MW/cm^2 range. Indeed, direct temperature measurements using liposomes labeled with a thermally sensitive fluorophore revealed a temperature increase of only approximately 1 $^\circ$C/100 mW[15].

In contrast, 760 nm radiation led in 90% of the investigated cells to significant autofluorescence changes. Previous work has shown that 760 nm microirradiation on glass-attached cells affects mitosis[10]. Interestingly, reduced hemoglobin exhibits a small absorption maximum at 760 nm (α= 4.5 cm^{-1})[16]. Therefore, heme-containing enzymes are possible absorbers. So far, no intracellular temperature measurements exist at this wavelength and the mechanism for autofluorescence changes could be photothermal or photochemical.

The most significant changes in autofluorescence occurred during UVA exposure even with 10^7 less intensity than the trapping beam. Efficient absorbers in this spectral region are endogenous porphyrins (including metallo-porphyrins), pyridine and flavin molecules. A significant decrease in autofluorescence down to 37% was detected at radiant exposures of 1-100 J/cm^2. Considering that some fading occurs during the initial measurement (1 s exposure time), the real decrease is probably be even greater. This initial fluorescence decrease may be explained by UVA-induced oxidation processes and, therefore, transformation into non-fluorescent NAD(P). This could occur via well-known type I and II photooxidation mechanisms (involving superoxide (O$_2$-) and singlet oxygen (^{1}O$_2$), respectively) where NAD(P)H and flavins act as photosensitizers[17,18].

Photogenerated oxygen species can cause oxidative stress and cell lysis by lipid peroxidation, membrane and DNA damage, and enzyme inactivation. It has been reported that NADH photosensitization plays a role in UV-induced DNA strand breaks[17,18]. Lubart et al.[19] found inhibition of cell mitosis after 360 nm exposure in the J/cm^2 range. In this paper, we observe that UV exposure with radiant exposures larger than 100 J/cm^2 results in a strong fluorescence increase (up to 550% of the initial value). These changes in fluorescence do not correlate with immediate visible morphological changes. Possible mechanisms for this signal increase may be photochemically-induced alterations in the cellular redox balance accompanied by elevated NADH levels, NADH efflux from defective mitochondria, and coenzyme binding with cytoplasmatic and nuclear proteins.

Liang et al.[20] recently investigated the effect of IR microirradiation on the nucleus of monolayers of CHO cells and found that cell division was inhibited for light exposures >10 GJ/cm^2. However to date, no studies exist regarding the cell division processes of trapped CHO cells. Further studies are necessary to correlate autofluorescence changes with cell damage in order to determine whether this is a useful probe of cell viability in an optical trap.

6. ACKNOWLEDGEMENTS

7. REFERENCES

1. A. Ashkin. "Acceleration and Trapping of Particles by Radiation Pressure", *Phys. Rev. Lett.* 24, 156-159, 1970.

2. A. Ashkin, JM. Dziedzic, JE Bjorkholm, S. Chu, "Observation of a single-beam gradient force optical trap for dielectric particles", *Opt. Lett.*, 11, 288-290,1986.

3. A.E. Siegman, "Lasers", University Science Books, Mill Valley, CA, 1986.

4. B. Chance and B. Thorell, "Localization and kinetics of reduced pyridine nucleotides in living cells by microfluorimetry.", *J. Biol. Chem.* 234, 3044-3050, 1959.

5. A. Mayevski, "Brain NADH Redox State Monitored In Vivo By Fiber Optic Surface Fluorometry", *Brain Res. Reviews* 7, 49-68, 1984.

6. W. Lohmann, "In situ detection of melanomas by fluorescence measurements", *Naturwissenschaften* 75, 201-202, 1988.

7. H. Schneckenburger, P. Gessler, I. Pavenstädt-Grupp, "Measurement of mitochondrial deficiencies in living cells by microspectrofluorometry", *J. Histochem. Cytochem.* 40(10), 1573-1578, 1992.

8. H. Schneckenburger and K. König, "Fluorescence decay kinetics and imaging of NAD(P)H and flavins as metabolic indicators", *Opt Eng.* 31(7), 1447-1451, 1992.

9. K. König, "In vivo autofluorescence measurements during photodynamic damage of cells and tumour tissue", In: W. Waidelich (ed.): *Laser. Optoelectronics in Medicine 1993.* In press.

10. IA. Vorobjev, H. Liang, WH. Wright, MW. Berns. "Optical trapping of chromosome manipulation: a wavelength dependence of induced chromosome bridges", *Biophys. J.* 64, 533-538, 1993.

11. G. Rose, "A separable and multipurpose tissue culture chamber", *Texas Rep. Biol. Med.* 12, 1074-1083, 1954.

12. W.H. Wright, G.J. Sonek, M.W. Berns, "Parametric study of the forces on microspheres held by optical tweezers", Appl. Optics 33, 1735-1748, 1994.

13. B. Liang and H. R. Petty, "Imaging Neutrophil Activation: Analysis of the Translocation and Utilization of NAD(P)H-Associated Autofluorescence during Antibody-Dependent Target Oxidation", *J. Cell. Phys.* 152, 145-156, 1992.

14. C. Y. Guezennec, F. Lienhard, F. Louisy, G. Renault, M.H. Tusseau, P. Portero, "In situ NADH laser fluorimetry during muscle contraction in humans", *Eur. J. Appl. Physiol.* 63, 36-42, 1991.

15. Y. Liu, D. Cheng, G.J. Sonek, B. J. Tromberg, and M.W. Berns, "A microspectroscopic technique for the determination of localized heating effects in organic particles", *Appl. Phys. Lett.* In press.

16. S. Wray, M. Cope, D.T. Delpy, J.S. Wyatt, E.O.R. Reynolds, "Characterization of the near-infrared absorption spectra of cytochrome aa3 and hemoglobin for the non-invasive monitoring of cerebral oxygenation", *Biochemica Biophysica Acta* 933, 184-192, 1988.

17. T.G. Burchuladze, E.G. Sideris and G.I. Fraikin, "Sensitized NADH formation of single-stranded breaks in plasmid DNA upon the action of near UV radiation", *Biofizika* 35, 722-725, 1990.

18. M.L. Cunningham, J.S. Johnson, S.M. Giovanazzi, and M.J. Peak, "Photosensitized production of superoxide anion by monochromatic (290-405 nm) ultraviolet irradiation of NADH and NADPH coenzymes", *Photochem. Photobiol.* 42(2), 125-128, 1985.

19. R. Lubart, Y. Wollman, H. Friedmann, S. Rochkind, and I. Laulicht, "Effects of visible and near-infrared lasers on cell cultures", *J. Photochem. Photobiol. B* 12, 305-310, 1992.

20. H. Liang, P. Krishnan, S. Cheng, K. Vu and M. Berns."Study on Cell Survival and Clonal Growth in CHO cells after Treatment of Laser Induced Optical Forces at various Near Infrared to Infrared Wavelengths on the Nucleus", submitted for publication.